


## Article

# Plasma Catalytic Conversion of CH<sub>4</sub> to Alkanes, Olefins and H<sub>2</sub> in a Packed Bed DBD Reactor

Mohammadreza Taheraslani <sup>1,2,\*</sup> and Han Gardeniers <sup>1</sup> 

<sup>1</sup> Mesoscale Chemical Systems, MESA+ Institute for Nanotechnology, University of Twente, P.O. Box 217, 7500 AE Enschede, The Netherlands; j.g.e.gardeniers@utwente.nl

<sup>2</sup> Faculty of Science and Technology, University of Twente, P.O. Box 217, 7500 AE Enschede, The Netherlands

\* Correspondence: m.taheraslani@utwente.nl

Received: 14 June 2020; Accepted: 28 June 2020; Published: 1 July 2020



**Abstract:** Methane is activated at ambient conditions in a dielectric barrier discharge (DBD) plasma reactor packed with Pd/ $\gamma$ -alumina catalyst containing different loadings of Pd (0.5, 1, 5 wt%). Results indicate that the presence of Pd on  $\gamma$ -alumina substantially abates the formation of deposits, leads to a notable increase in the production of alkanes and olefins and additionally improves the energy efficiency compared to those obtained for the non-packed reactor and the bare  $\gamma$ -alumina packed reactor. A low amount of Pd (0.5 and 1 wt%) favors achieving a higher production of olefins (mainly C<sub>2</sub>H<sub>4</sub> and C<sub>3</sub>H<sub>6</sub>) and a higher yield of H<sub>2</sub>. Increasing Pd loading to 5 wt% promotes the interaction of H<sub>2</sub> and olefins, which consequently intensifies the successive hydrogenation of unsaturated compounds, thus incurring a higher production of alkanes (mainly C<sub>2</sub>H<sub>6</sub> and C<sub>3</sub>H<sub>8</sub>). The substantial abatement of the deposits is ascribed to the role of Palladium in moderating the strength of the electric and shifting the reaction pathways, in the way that hydrogenation reactions of deposits' precursors become faster than their deposition on the catalyst.

**Keywords:** methane activation; plasma catalysis; C<sub>2</sub> hydrocarbons; dielectric barrier discharge; hydrogenation

## 1. Introduction

Non-thermal plasma techniques have extensively been employed for the production of value-added products, including hydrogen, hydrocarbons, oxygenates (e.g., methanol) and aromatics, at ambient conditions [1]. Operating at ambient conditions gives a unique opportunity in order to take advantage of non-thermal plasma to transfer electrical energy to chemical energy using high-energy electrons to activate stable molecules, such as methane. However, the gas-phase plasma reactions occur via a free radical mechanism [2] and may not be efficiently selective to desired products. In a plasma-catalyst hybrid system, reactive plasma species (e.g., radicals) can interact with the catalyst, which can influence the reaction pathways and the selectivity of the desired products [3–13]. The plasma provides the required energy for activation of the stable molecule by breaking the bond (e.g., C-H for methane activation) and generates a pool of radicals, which can react with the catalyst, as the medium that is capable of conducting the interaction among radicals, selectively shifting reaction pathways towards more value-added products.

For methane activation, plasma generates CH<sub>x</sub> fragments and H radicals, for which their successive recombination and interactions lead to the formation of higher hydrocarbons and hydrogen, while deposits also form as the by-product. The introduction of a packing material inside the plasma discharges can shift the distribution of products. Several catalyst-supports, such as alumina, silica and titania [7,14,15], with or without metals, such as Pt, Ni, Cu and Ru, were utilized for conversion of methane via a non-oxidative route in combination with dielectric barrier discharge (DBD) plasma

reactors [8,10,16–18]. Previous studies focused on the investigation of methane activation to higher hydrocarbons, where the separate role of metal and catalyst support and their synergy with DBD plasma was not fully clarified [17]. In addition, the formation of deposits can be influenced by the presence of metal on a surface of a dielectric catalyst support, which has been reported in the previous studies; however, it was not discussed how the interaction of a catalyst support (e.g., alumina) or a metal supported catalyst (e.g., Pd/alumina) with plasma species can increase or decrease the formation of deposits and change the formation of C<sub>2</sub> and C<sub>3</sub> compounds. Therefore, the synergy between the catalyst support and the metal supported catalyst with the DBD plasma discharges for methane activation needs to be studied, as it can highly influence the distribution of products.

In the present study, the interaction of DBD plasma species with  $\gamma$ -alumina and Palladium-loaded  $\gamma$ -alumina with different loadings of Pd is investigated. The synergy between plasma and catalyst is discussed in terms of methane conversion, selectivity of C<sub>2</sub> compounds and the selectivity of deposits. It is discussed how the presence of Palladium impacts the properties of discharges and shifts the reaction pathways, substantially changing the distribution of products and the formation of deposits. The involved radical chemistry and the interactions of plasma-generated radicals with the Pd catalyst are furthermore elaborated. The energy efficiency is evaluated for the comparison of the results for the non-packed reactor and the reactor packed with Pd catalyst. Finally, the synergistic integration of Pd/alumina catalyst with DBD discharges for methane activation is represented in terms of the investigated parameters.

## 2. Results and Discussion

### 2.1. The Plasma Electrical Parameters

The average applied voltages utilized during the plasma reaction for the blank DBD reactor and the packed DBD reactor are represented in Table 1.

**Table 1.** Applied voltage and breakdown voltage for the non-packed reactor (Blank) and the packed reactor.

Experiment	Blank	$\gamma$ -alumina	0.5%Pd/ $\gamma$ -alumina	1.0%Pd/ $\gamma$ -alumina	5.0%Pd/ $\gamma$ -alumina
Applied Voltage (kV)	7.6	9.0	9.0	8.9	8.8
Breakdown Voltage (kV)	1.9	1.7	1.8	1.9	2.1

A higher voltage of 8.8–9.0 kV is required when the plasma gap is packed with the catalyst, in comparison with the value of the voltage applied for the non-packed reactor (7.6 kV), in order to obtain the same value, of 7–8 W, as the output power. Furthermore, the breakdown voltage (i.e., obtained from the Lissajous Figures, depicted in Figure 1 changes as the discharge gap is filled by catalyst particles, lowering the space for the propagation of plasma discharges [19–21]. Figure 1 depicts the Lissajous Figures for the blank reactor and the packed reactor with  $\gamma$ -alumina and Pd-loaded  $\gamma$ -alumina. The typical shift for the shape of the Lissajous Figure from parallelogram (i.e., for the non-packed reactor) to an almond shape (i.e., for the packed reactor) was obtained. Packing the discharge gap with catalyst particles changes the filamentary formation of discharges into more of a formation of surface discharges than filamentary discharges [22,23].

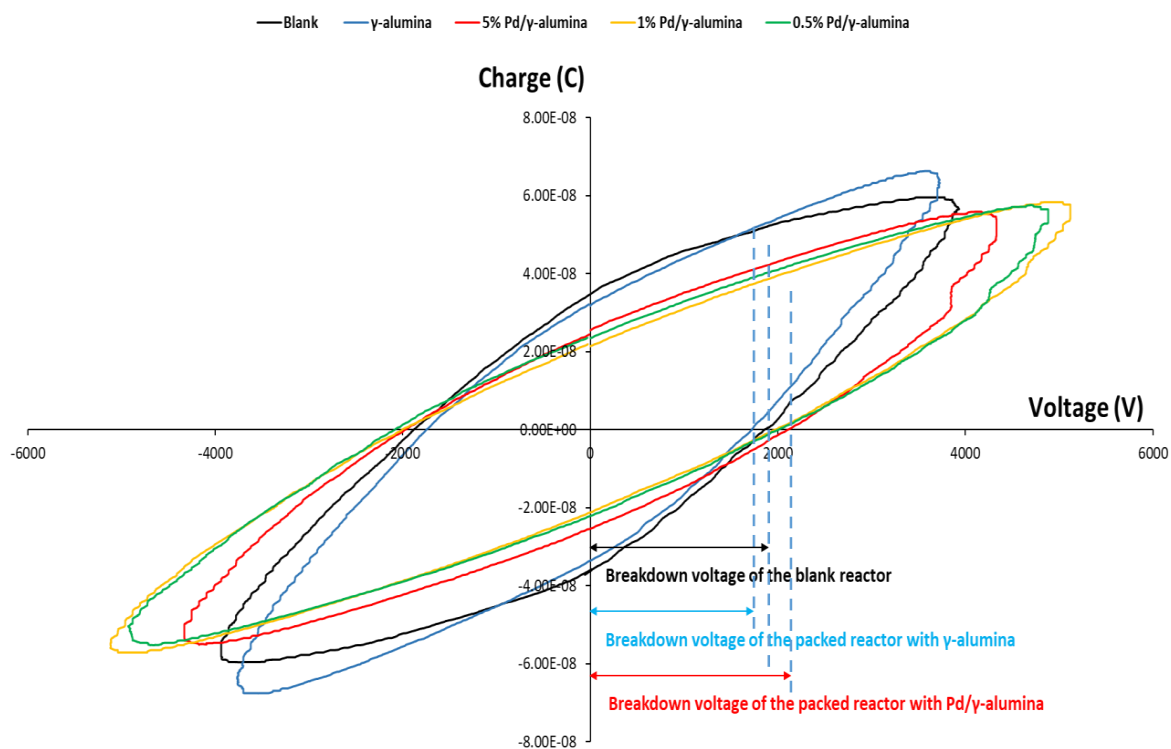


Figure 1. Effect of the catalyst on Lissajous figures.

The values obtained for the packed reactor indicate that the breakdown voltage can be influenced by the conductivity of the catalyst. As can be seen in Table 1, the breakdown voltage follows an ascending trend by the increase of the Pd content. This indicates that the presence of conductive Palladium reduces the capacitance of the catalyst bed and thus it demands a higher breakdown voltage to ignite the plasma. On the other hand, the conductivity of Pd particles induces a higher amount of charge to be transferred across the catalyst bed, which moderates the strength of the electric field to a rather weaker electric field than the non-conductive, bare,  $\gamma$ -alumina packed reactor. Thus, a lower strength of the electric field causes a lower level of energy absorbed by  $\text{CH}_4$  molecules and a lower conversion for the Pd/ $\gamma$ -alumina packed reactor. This will be discussed in the following section in combination with the conversion and the selectivity of the products.

## 2.2. The Conversion of Methane and the Selectivity of Products

Figure 2 represents the conversion of methane and the selectivity of  $\text{C}_2$  products for the DBD plasma reactor packed with  $\gamma$ -alumina and Pd/ $\gamma$ -alumina with different loadings of Pd (0.5, 1, 5 wt%). Packing bare  $\gamma$ -alumina inside the plasma discharges improves the conversion of methane in comparison with the blank DBD plasma reactor. This occurs due to the accumulation of high-energy electrons on the surface, in particular near contact points of particles, where the gap space becomes smaller. In this way, the energy absorbed in plasma discharges increases, and consequently, a higher amount of energy is transferred to methane molecules, which leads to a higher conversion of methane. However, this improvement changes with time, as can be seen in Figure 2a, because of the formation of deposits on the surface of  $\gamma$ -alumina [16,24,25]. The formation of deposits, which contains conductive carbon species, influences the electrical impedance of the DBD reactor, by short-circuiting the electric field across the  $\gamma$ -alumina particles, leading to a relatively lower strength of the electric field, and thus, a descending trend for the conversion of methane is obtained during the reaction time. As can be seen in Figure 1, for the 5 wt% Pd/ $\gamma$ -alumina packed reactor, the initial activity is lower than other experiments and it raises by proceeding the reaction time. This can be related to the conductivity of Palladium and its higher breakdown voltage in comparison with other packed reactors and the

non-packed reactor. In this case, a higher voltage for the 5 wt% Pd/ $\gamma$ -alumina packed reactor should be applied to ignite the plasma. Consequently, a longer time is expected for the expansion and the establishment of the plasma discharges to be developed across the catalyst bed. As a result, a weaker electric field is formed at the beginning of the reaction.

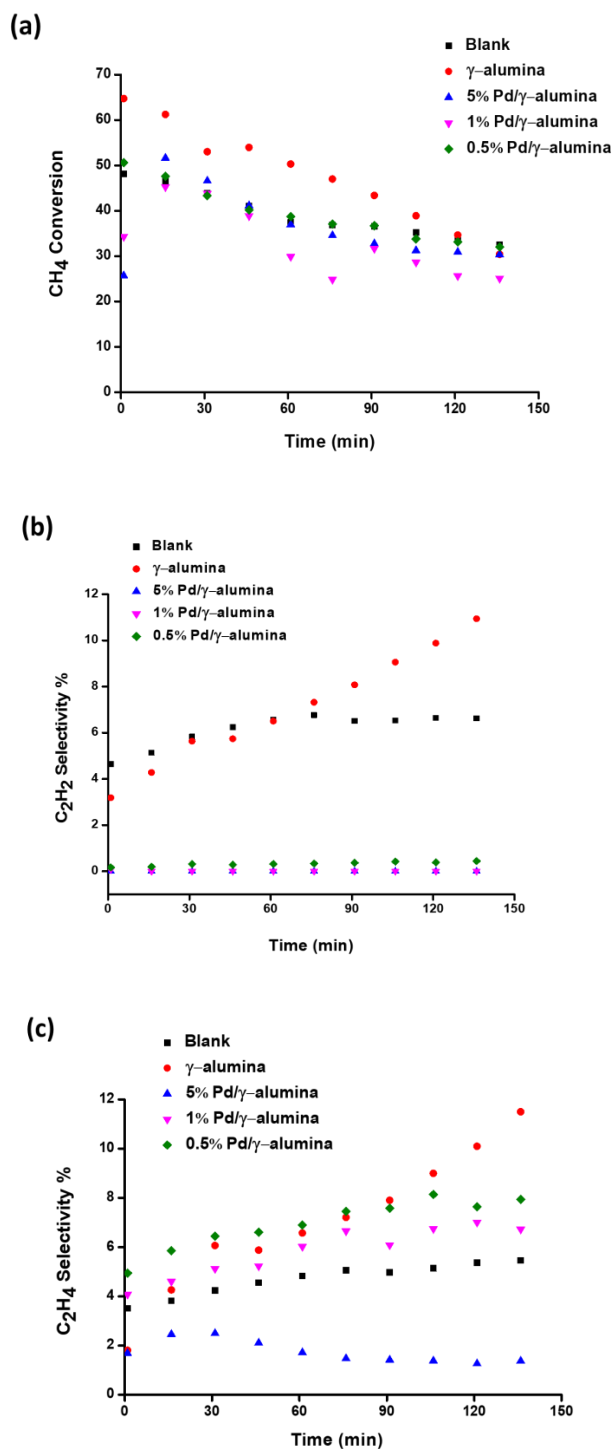
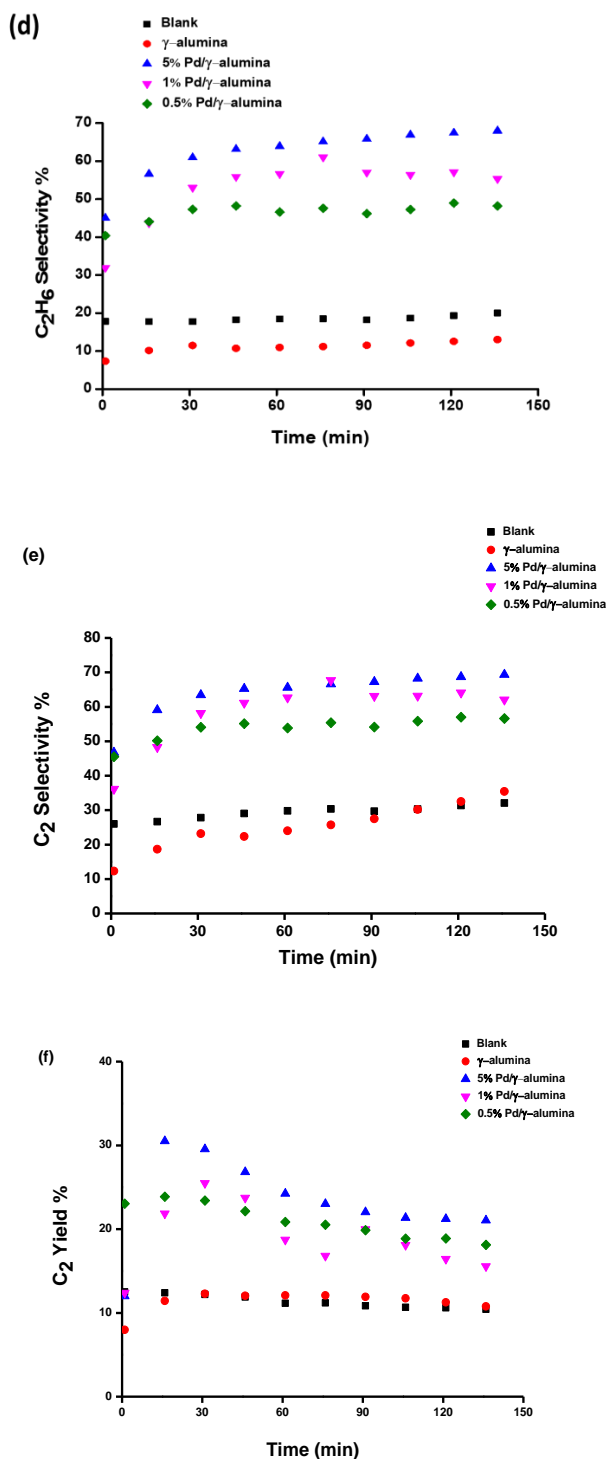


Figure 2. Cont.



**Figure 2.** Effect of packing the dielectric barrier discharge (DBD) plasma reactor with  $\gamma$ -alumina and Pd/ $\gamma$ -alumina with different loadings of Pd (0.5, 1, 5 wt%): (a) methane conversion, (b) acetylene selectivity, (c) ethylene selectivity, (d) ethane selectivity, (e) C<sub>2</sub> selectivity, (f) C<sub>2</sub> yield.

Gadzhieva et al. [26] studied the dissociation of methane in a plasma-induced medium, packed with  $\gamma$ -alumina using diffuse scattering infrared (IR) spectroscopy. In agreement with the results of the present study,  $\gamma$ -alumina showed a positive effect in enhancing the conversion of methane; however, for a longer exposure time of  $\gamma$ -alumina to methane plasma, the transmittance of the IR system weakened due to the formation of deposits. It was explained that the exposure of  $\gamma$ -alumina to plasma discharges generates new active sites for adsorption of excited methane. These active sites are capable to store the

energy of plasma components (e.g., electrons, radicals, ions) and to transfer the energy to methane molecules. Thus, methane is dissociated into  $\text{CH}_x$  fragments with a higher conversion, in comparison with using only plasma activation. However, their results indicate a more dominant effect of  $\gamma$ -alumina as a dielectric material, with the capability of intensifying the electric field rather than as a catalyst.

This becomes a different case when Pd particles are dispersed on  $\gamma$ -alumina. Although the presence of Pd increases the conductivity of the catalyst, Pd catalytic activity greatly influences the distribution of products. Figure 2b, c and d depict the selectivity of  $\text{C}_2$  compounds. In the case of packing with  $\gamma$ -alumina, the distribution of  $\text{C}_2$  products shifts towards a higher formation of unsaturated compounds, like  $\text{C}_2\text{H}_2$  and  $\text{C}_2\text{H}_4$ . The recombination reactions of  $\text{CH}_x$  radicals (i.e., generated by dissociation of methane) are the predominant routes for the production of  $\text{C}_2$  compounds, like  $\text{C}_2\text{H}_2$ ,  $\text{C}_2\text{H}_4$  and  $\text{C}_2\text{H}_6$  [27–29]. However, the distribution of  $\text{CH}_x$  fragments ( $\text{CH}_3$ ,  $\text{CH}_2$ ,  $\text{CH}$ ,  $\text{C}$ ) is influenced by the presence of a metal (Pd) on the surface of a dielectric material ( $\gamma$ -alumina). For the  $\gamma$ -alumina packed reactor, the higher formation of  $\text{C}_2\text{H}_2$  and  $\text{C}_2\text{H}_4$  implies that a higher concentration of  $\text{CH}_2$  and  $\text{CH}$  are generated at the presence of  $\gamma$ -alumina inside the discharges. This changes when Pd is introduced to the system, owing to the capability of Pd in enhancing the hydrogenation reactions. Highly reactive radicals (e.g.,  $\text{CH}_2$ ,  $\text{CH}$ ) and unsaturated compounds (e.g.,  $\text{C}_2\text{H}_4$ ,  $\text{C}_2\text{H}_2$ ) go through Pd-catalyzed hydrogenation reactions, which leads to a substantial increase in the formation of  $\text{CH}_3$  radicals, which subsequently recombine to form  $\text{C}_2\text{H}_6$ . However, the distribution of  $\text{C}_2$  compounds is strongly impacted by the amount of Pd loading. For 1 and 5 wt% loading of Palladium, no  $\text{C}_2\text{H}_2$  is formed. This changes when the amount of Pd loading lowers to 0.5 wt%, resulting in a higher production of  $\text{C}_2\text{H}_2$ . According to Figure 3c, the selectivity of  $\text{C}_2\text{H}_4$  is higher for Pd loadings of 0.5 and 1 wt%. Increasing the amount of palladium loading to 5 wt% provides more active sites for successive hydrogenation of unsaturated compounds. As a result, both  $\text{C}_2\text{H}_2$  and  $\text{C}_2\text{H}_4$  compounds go through hydrogenation reactions to form  $\text{C}_2\text{H}_6$ . In order to further clarify the effect of Palladium, the selectivity of  $\text{C}_2$  as well as the yield of  $\text{C}_2$  products are shown in Figure 2e,f, respectively. Both figures clearly demonstrate the improvement of the production of  $\text{C}_2$  compounds for Pd-loaded  $\gamma$ -alumina catalysts in comparison with the non-packed reactor and the packed reactor with bare  $\gamma$ -alumina. The improvements show stability during the reaction time.

Figure 3 shows the selectivity of  $\text{C}_3$  and  $\text{C}_{4+}$  products. For the bare  $\gamma$ -alumina packed reactor, the formation of  $\text{C}_3\text{H}_6$  is higher. Following a similar trend as the  $\text{C}_2$  compounds, a higher production of  $\text{C}_3\text{H}_8$  is obtained for Pd-loaded  $\gamma$ -alumina compared to the  $\gamma$ -alumina packed reactor, taking place via the hydrogenation reaction of  $\text{C}_3\text{H}_6$  to  $\text{C}_3\text{H}_8$ .

The selectivity of larger hydrocarbons ( $\text{C}_{4+}$ ) is depicted in Figure 3. According to these results, a lower amount of  $\text{C}_{4+}$  is produced when  $\gamma$ -alumina and Pd/ $\gamma$ -alumina are packed in the reactor. The lower formation of  $\text{C}_{4+}$  is in line with a higher formation of  $\text{C}_2$  compounds. This can be explained by the effect of packing on the distribution of primary radicals ( $\text{CH}_3$ ,  $\text{CH}_2$  and  $\text{CH}$ ) as well as secondary radicals ( $\text{C}_2\text{H}$ ,  $\text{C}_2\text{H}_3$  and  $\text{C}_2\text{H}_5$ ). The  $\text{C}_3$  and  $\text{C}_{4+}$  products are formed by the reactions between  $\text{CH}_x$  and  $\text{C}_2\text{H}_y$  radicals. These reactions are terminated by the catalyst in a way that it reduces the formation of  $\text{C}_{4+}$  products. This is attributed to the surface reactivity of Pd/ $\gamma$ -alumina, which enhances the interaction of  $\text{CH}_x$  and  $\text{C}_2\text{H}_y$  radicals with the catalyst surface, terminating the reaction pathways towards more  $\text{C}_2$  and  $\text{C}_3$  products. In other words, most radical chain reactions terminate before they go through further interactions between  $\text{C}_2$  and  $\text{C}_3$  species for generating larger hydrocarbons.

The selectivity of deposits and the yield of hydrogen are shown in Figure 4. A higher formation of deposits is obtained for the  $\gamma$ -alumina packed reactor, which corresponds with a higher conversion of methane (depicted in Figure 3a) and a higher yield of  $\text{H}_2$ , generated by  $\text{CH}_4$  dissociation to  $\text{CH}_x$  and  $\text{H}$  radicals. Although a stronger electric field is formed for the  $\gamma$ -alumina packed reactor, the extra energy of the formed electric field is mainly consumed for a higher production of deposits.

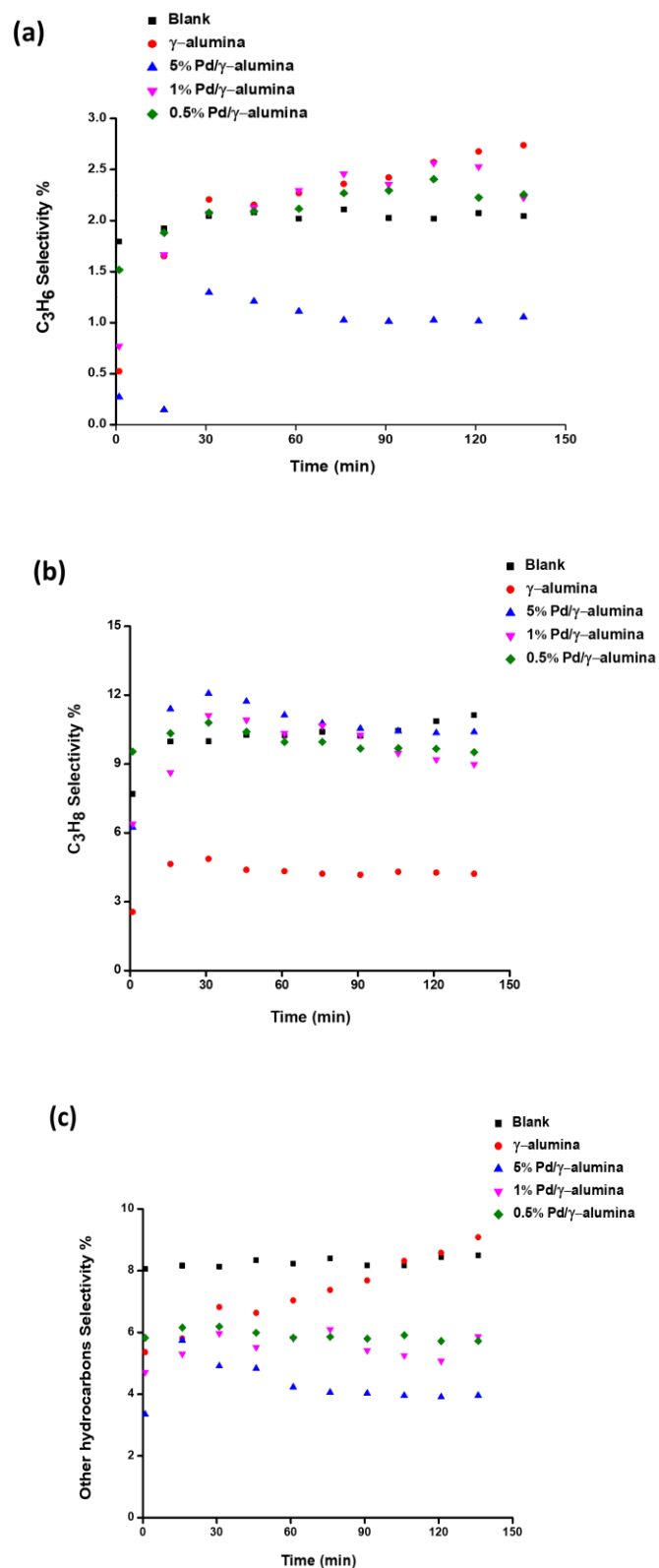


**Figure 3.** The effect of packing the DBD plasma reactor with  $\gamma$ -alumina and Pd/ $\gamma$ -alumina with different loadings of Pd (0.5, 1, 5 wt%): (a) propylene selectivity, (b) propane selectivity, (c) other hydrocarbons' selectivity.

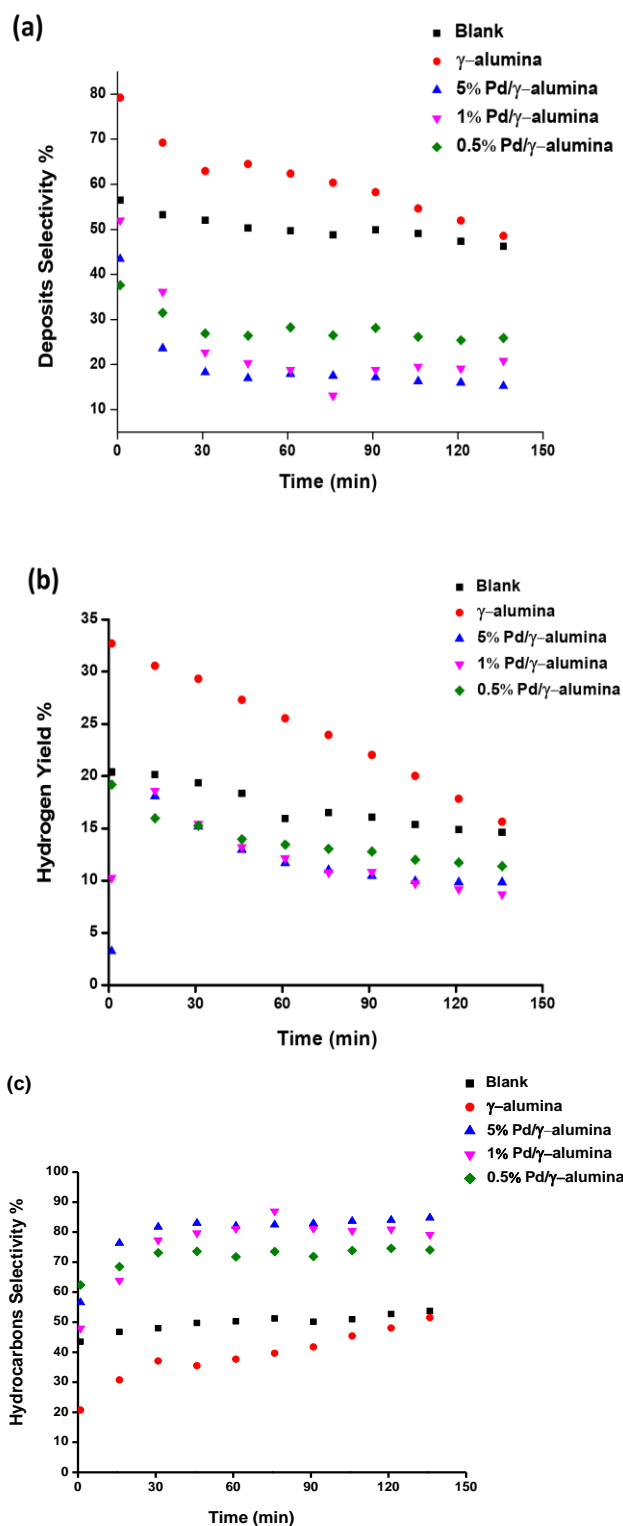


**Figure 4.** The effect of packing the DBD plasma reactor with  $\gamma$ -alumina and Pd/ $\gamma$ -alumina with different loadings of Pd (0.5, 1, 5 wt%) on the DBD plasma reactor: (a) deposits selectivity, (b) hydrogen yield, (c) hydrocarbons selectivity.

The selectivity of deposits remarkably decreases with the presence of Pd on  $\gamma$ -alumina, accompanied with a lower yield of  $H_2$  for Pd/ $\gamma$ -alumina catalysts. This is in line with the increase in the selectivity of all hydrocarbons ( $C_{2+}$ ), as shown in Figure 4c. In addition, the improvement of the formation of hydrocarbons show a stable manner during the reaction, with a noticeable gap between



the results obtained for the Pd-loaded  $\gamma$ -alumina packed reactor, in comparison with the non-packed reactor and the bare  $\gamma$ -alumina packed reactor. Furthermore, the results indicate that even with a low amount of Pd, the formation of deposits is noticeably reduced. The lowest selectivity of deposits was 15%, achieved for Pd/ $\gamma$ -alumina with 5 wt% of Pd loading, significantly lower than that obtained for the blank reactor (47%).

Results indicate that, in addition to the effect of Pd in reducing deposits, it can tune the distribution of alkanes and olefins. For instance, the formation of  $C_2H_4$  becomes greater than that obtained for the blank reactor, when Pd/ $\gamma$ -alumina with 1 wt% of Pd loading is used as the catalyst, while the formation of deposits has substantially been abated. Increasing Pd loading to 5 wt% hydrogenates  $C_2H_4$  to  $C_2H_6$ . According to the presented results, 1 wt% Pd/ $\gamma$ -alumina is considered as the optimum catalyst for a higher production of  $C_2H_4$  and  $C_2H_6$ , as well as for its resistance to the formation of deposits.

Figure 5 shows the dielectric quartz tube after the experiments performed in the blank and the packed reactors. For the blank reactor, the formation of deposits was mainly observed on the inner surface of the dielectric quartz tube [30]. For the  $\gamma$ -alumina packed reactor, the yellowish deposits were still formed on the inner surface of the quartz tube. As can be seen in Figure 5c–e, for Pd-loaded  $\gamma$ -alumina, the formation of deposits is not observed, indicating a noticeable decrease in the formation of deposits, which is in line with the results obtained for the selectivity of the products.

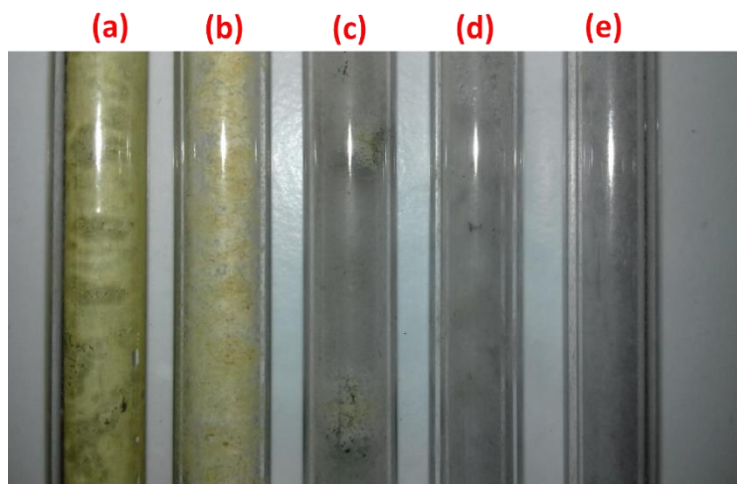


**Figure 5.** Formation of deposits on the inner surface of the dielectric quartz tube after plasma reaction: (a) the blank reactor, (b) the packed reactor with  $\gamma$ -alumina, (c) the packed reactor with 0.5 wt% Pd/ $\gamma$ -alumina, (d) the packed reactor with 1.0 wt% Pd/ $\gamma$ -alumina, (e) the packed reactor with 5.0 wt% Pd/ $\gamma$ -alumina.

### 2.3. The Energy Consumption Analysis

#### 2.3.1. The Effect of Specific Energy Input (SEI)

In order to compare the performance of the blank and the packed reactor, the conversion of methane and the yield of  $C_2$  and deposits are evaluated versus specific energy input, as shown in Figure 6. The specific energy input (SEI) is defined as the ratio of the discharge power to the total flow rate of the gas stream.

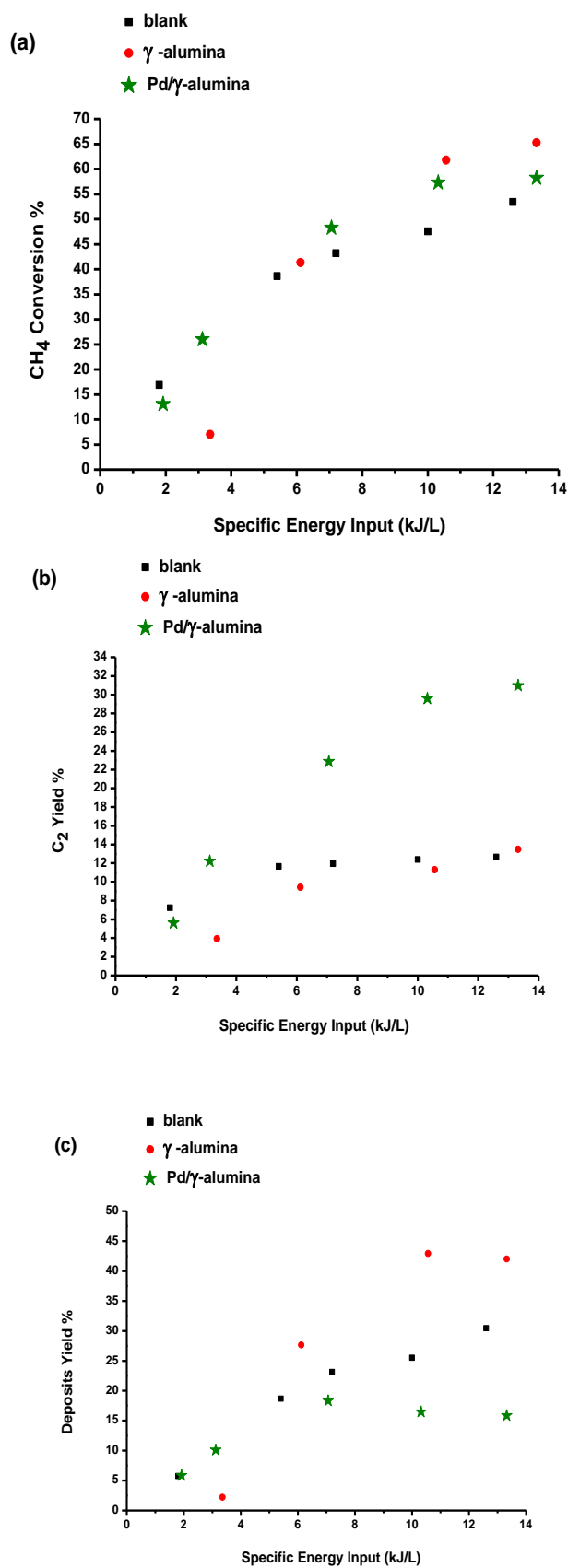


**Figure 6.** (a) Conversion of methane, (b) the yield of C<sub>2</sub> compounds and (c) the yield of deposits versus specific energy input for the blank reactor and the packed reactor with  $\gamma$ -alumina and 1 wt% Pd/ $\gamma$ -alumina.

As can be seen in Figure 6a, the conversion of methane increases for both the blank reactor and the packed reactor, by increasing the specific energy input (SEI). For a SEI below 4 kJ/L, the conversion of methane for the packed reactor is lower than that in the blank reactor. The reason is attributed to the presence of the catalyst and its impact on the formation of discharges, which is called the “partial discharging” [21–23], occurring in packed bed DBD reactors. In addition, the energy provided at low SEIs is not sufficient to propagate the discharges across the catalyst bed. In other words, plasma discharges do not entirely develop through the whole spaces of the discharge gap and some spaces remained unfilled. As a result, at low SEIs, a weaker electric field forms for the packed reactor, which results in a lower amount of discharge power, causing a lower conversion of methane. In contrast, at higher values of SEIs, when a SEI of more than 8 kJ/L is applied for the packed reactor, the conversion of methane is promoted to higher values than the non-packed reactor. By increasing the specific energy input to values greater than 12 kJ/L, the conversion of methane for the packed reactor reaches 70% for  $\gamma$ -alumina and 58% for Pd/ $\gamma$ -alumina, which is higher than the conversion value of 53% obtained for the blank reactor. It should be noted that the specific energy input parameter covers both the discharge power and the residence time in its definition. This can be deduced from Figure 6, where a longer residence time implies a lower flow rate, which corresponds with a higher value for the specific energy input. In this case, the effect of residence time can be anticipated, where a longer exposure of the reactant to plasma discharges can intensify the interaction of plasma species and the catalyst, which can result in a higher conversion of  $\text{CH}_4$ , and accordingly, a higher formation of  $\text{C}_2$  products for the Pd/ $\gamma$ -alumina packed reactor, while the formation of deposits is mitigated.

The results indicate that a stronger electric field can be formed when  $\gamma$ -alumina is packed inside the discharge gap, achieving a higher conversion of methane in comparison with the Pd-loaded catalyst. However, the higher formation of deposits for the  $\gamma$ -alumina gradually reduces the strength of the electric field and results in a lower conversion. On the other hand, the presence of Pd on  $\gamma$ -alumina introduces a conductive surface to the plasma discharges, which therefore moderates the strength of the electric field for the Pd/ $\gamma$ -alumina packed bed reactor. Similar results have been obtained for other conductive metals, such as Pt [17,31] and Ni [32,33], which could moderate the strength of the electric field. Although the moderation of the electric field yields to a rather lower conversion of methane,  $\text{C}_2$  yield (Figure 6b) is substantially improved, due to the noticeable reduction in the formation of deposits (Figure 6c).

For Pd/ $\gamma$ -alumina,  $\text{C}_2$  yield increases by increasing SEI, where it reaches to 31% for a SEI of 13 kJ/L. In contrast, for the blank reactor and the packed reactor with  $\gamma$ -alumina,  $\text{C}_2$  yield shows slight changes by increasing SEI, whereas  $\text{C}_2$  yield slightly increases from 10% to 14% when SEI increases more than two times, from 6 kJ/L to 13 kJ/L. Applying a SEI value of more than 7 kJ/L results in a much higher yield of  $\text{C}_2$  (31%), while the deposits yield remains almost constant at 16%. In contrast, the deposits yield for the blank reactor and for the packed reactor with  $\gamma$ -alumina shows an ascending trend by increasing SEI, nearly proportional to the trend obtained for the conversion of methane.

### 2.3.2. The Energy Efficiency

The energy efficiency versus different specific energy inputs (SEI) is shown in Figure 7. These values were calculated by considering the high heat value (HHV) of the products and methane and the discharge power applied for the performed experiments, according to the following equation:

$$\text{Energy Efficiency \%} = \frac{\sum_{i=\text{product}}^n \text{HHV}(i) \times \text{molar flow rate}(i)}{\text{HHV of CH}_4 \times \text{molar flow rate of reacted CH}_4 + \text{Discharge Power}} \times 100$$

where,  $i$  = product and  $\text{HHV}(i)$  = high heat value of  $i$  (J/mol), with molar flow rate of  $i$  (mol/s) and discharge power (Watt).

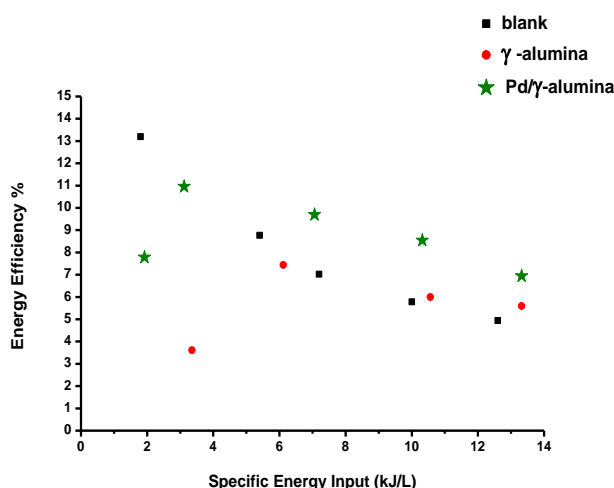


**Figure 7.** Energy efficiency versus specific energy input for the blank reactor and the packed reactor with  $\gamma$ -alumina and 1 wt% Pd/ $\gamma$ -alumina. Total flow rate = 50 ml/min,  $f$  = 23 kHz.

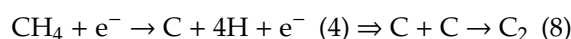
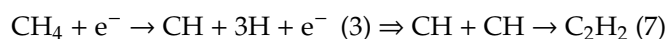
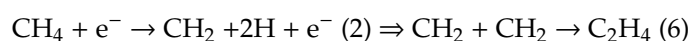
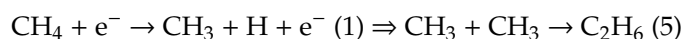
For both the blank reactor and the packed reactor, energy efficiency tends to decrease by increasing SEI. In a low SEI of 2 kJ/L, the energy efficiency of the blank reactor is 13%, which is higher than that obtained for the packed reactor (8%). However, in a low SEI, the values for the conversion of methane and the yield of  $C_2$  are very low, which is not favorable for the productivity of the reaction. Increasing SEI to higher values ( $\geq 4$  kJ/L) causes a remarkable drop in the energy efficiency of the blank reactor, where it reaches 5% in a SEI of 13 kJ/L.

For the packed reactor, the energy efficiency improves for SEI values higher than 4 kJ/L. However, the effect of packing in enhancing the energy efficiency becomes greater for Pd/ $\gamma$ -alumina, due to the presence of Pd, which not only improves the yield of  $C_2$  products and reduces the formation of deposits, but also enhances the energy efficiency of the plasma reaction compared to the non-packed reactor.

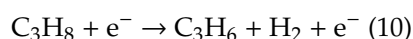
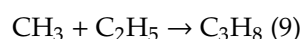
#### 2.4. Reaction Pathways

Dissociation of  $CH_4$  molecules in dielectric barrier plasma discharges is initiated by simultaneous production of  $CH_3$ ,  $CH_2$ ,  $CH$  and  $C$  radicals, as shown in reactions 1–4 [34].  $CH_x$  radicals go through radical chain reactions by recombination to produce  $C_2$  compounds, following the reactions 5–8 [35], presented below:

Electron impact dissociation: Recombination:



Further radical chain reactions occur inside the plasma discharges to form  $C_3$  compounds via interactions of primary radicals (e.g.,  $CH_3$ ) and secondary radicals (e.g.,  $C_2H_5$ ) as specified in reactions 9 and 10:



Subsequently, interactions of primary radicals with  $C_2$  and  $C_3$  radicals in plasma discharges produce  $C_{4+}$  hydrocarbons. The contribution of  $C_3$  and  $C_{4+}$  compounds in final products is smaller than that of  $C_2$  products.

Further radical chemistry can be involved in the production of products, as explained in previous studies [34,36].  $C_2$  compounds are the main products of the DBD plasma activation of methane and therefore the predominant reaction pathways for the production of  $C_2$  products are explained in the present study, as shown in Figure 8. Each color represents the type of the reaction which occurs within the pool of radical interactions. It should be emphasized that all involved reactions for the production of  $CH_x$  and  $C_2H_y$  species can be reversible, as shown in Figure 8 by the double headed arrows.

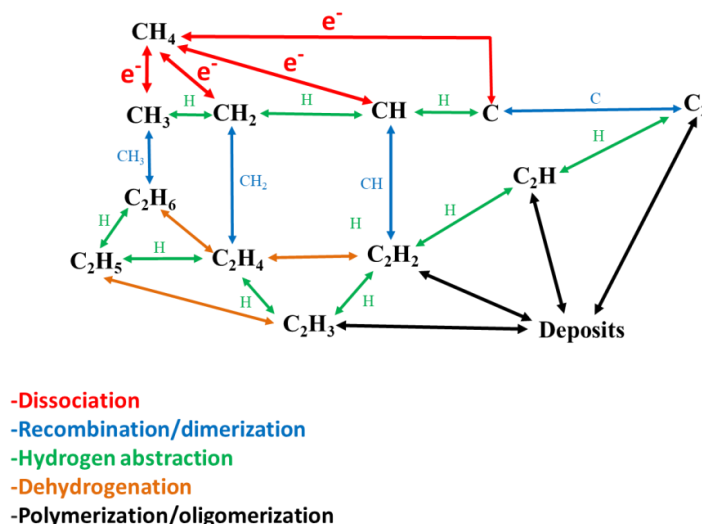


**Figure 8.** Proposed reaction pathways and radical reactions in coupling of methane to  $C_2$  and deposits in the DBD plasma reactor.

Different types of plasma species (e.g., radicals, ions, atoms) are generated when methane is activated by plasma. Among all generated species, radicals have a key role in determining the reaction pathways and the distribution of products. The activation of methane starts with electron impact dissociation to generate  $CH_x$  fragments, depicted in red in Figure 8.  $CH_x$  fragments go through recombination/dimerization reactions, which produce  $C_2H_6$ ,  $C_2H_4$  and  $C_2H_2$  products. In addition to the dimerization of  $CH_2$  and  $CH$  radicals to form  $C_2H_4$  and  $C_2H_2$ , successive dehydrogenation reactions of  $C_2H_6$  are also possible intermediate steps in the formation of  $C_2H_4$  and  $C_2H_2$ . On the other hand,  $C_2H_4$  and  $C_2H_2$  are unsaturated hydrocarbons that are considered as potentially reactive molecules. Thus, they can be the precursors for the formation of deposits. This can take place via the H abstraction from  $C_2H_4$  and  $C_2H_2$ , generating  $C_2H_3$  and  $C_2H$  intermediates, which subsequently contributes to the formation of deposits via polymerization/oligomerization reactions, as depicted in black in Figure 8.

At the presence of the catalyst packed inside the discharges, the strength of the electric field is altered, in which a different distribution of energy results in a different concentration of  $CH_x$  fragments, leading to a different pool of products. For the  $\gamma$ -alumina packed reactor, the selectivities of  $C_2H_2$  and  $C_2H_4$  are higher than that obtained for the blank reactor, which is attributed to the formation of a stronger electric field. For the Pd/ $\gamma$ -alumina packed reactor, the formation of deposits substantially reduces, accompanied with a notable increase for the yield of  $C_2$  products. Palladium catalyst promotes the hydrogenation reactions at ambient conditions, by adsorbing molecular  $H_2$  and unsaturated compounds (e.g.,  $C_2H_4$ ,  $C_2H_2$ ), as well as adsorbing the intermediates (e.g.,  $C_2H_5$ ,  $C_2H_3$ ,  $C_2H$ ) and H radicals. In other words, the presence of Pd catalyst intensifies the adsorption of H radicals, forming strong palladium–hydrogen bonds [37]. As a consequence, the intermediate species react with the adsorbed H radicals, promoting hydrogenation reactions faster than their oligomerization/polymerization to deposits. Furthermore, the amount of Pd loading can shift the distribution of  $C_2$  products, whereas a higher amount of Pd (5 wt%) is favorable for a higher degree of hydrogenation reactions, as it consumes a greater amount of unsaturated  $C_2$  compounds to form  $C_2H_6$ . The results indicate that hydrogenation

reactions follow a cascade trend, by which  $C_2H_2$  is first consumed to form  $C_2H_4$ , and subsequently,  $C_2H_4$  is hydrogenated to  $C_2H_6$ .

The mechanism of catalytic coupling of methane to  $C_2$  products in the Pd/ $\gamma$ -alumina packed reactor is shown in Figure 9. This mechanism is initiated by plasma activation of  $CH_4$  molecules, which generates  $CH_x$  radicals, and they recombine to form  $C_2H_y$  species. Subsequently, the generated  $CH_x$  and  $C_2H_y$  radicals interact with the catalyst. The interactions initiate with the adsorption of  $CH_x$  and  $C_2H_y$  plasma species on the surface. At the next step, the adsorbed radicals react on the Pd catalyst, going through recombination and/or hydrogenation reactions. Subsequently, the intermediates and the formed  $C_2$  compounds desorb to the gas phase. On the other hand, the adsorbed  $C_2H$  and  $C_2H_3$  can go through oligomerization/polymerization reactions, which then leads to the formation of deposits on the catalyst. In other words, the surface reactions can be competitive, in a way that the rate of hydrogenation and recombination of radicals ( $CH_x$ ,  $C_2H_y$ ), as well as the potentially reactive molecules (i.e.,  $C_2H_2$  and  $C_2H_4$ ), is competing with the rate of their oligomerization/polymerization reactions. The results indicate that Pd has a positive effect on enhancing the rate of hydrogenation/recombination reactions, faster than the rate of oligomerization/polymerization reactions, which reduces the formation of deposits.

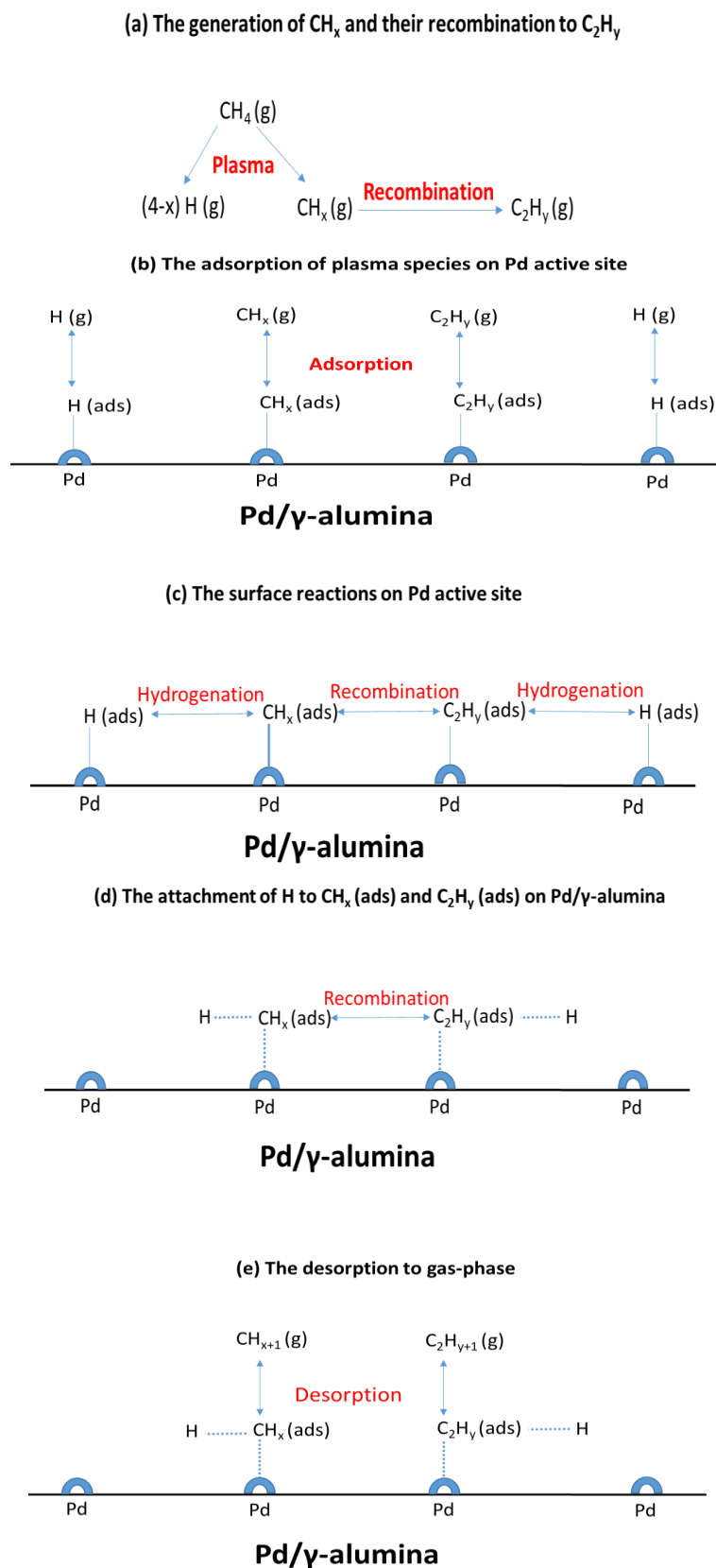
### 2.5. The Synergy of the Plasma and the Pd/ $\gamma$ -alumina Catalyst

Table 2 summarizes the performance of the non-packed DBD reactor and the packed DBD reactor, implemented in the present study.

**Table 2.** The effect of packing on the performance of the DBD plasma reactor for the present study, performed in specific energy input of 10–12 kJ/L.

Experiment	$CH_4$ Conversion %	$C_2$ Yield %	Deposits Yield %	Energy Efficiency %
The non-packed reactor	48%	12.4%	25.5%	5.8%
The $\gamma$ -alumina packed reactor	62%	11.3%	42.9%	6.0%
The Pd/ $\gamma$ -alumina packed reactor	57%	29.6%	16.5%	8.6%

The results indicate that the presence of a packing inside the discharge gap influences the plasma characteristics as well as the mechanism of the plasma discharges formation, as discussed in the previous sections. It was revealed that the conductivity of the catalyst influences the formation and expansion of plasma discharges, whereas the presence of Pd-conductive particles on  $\gamma$ -alumina moderates the electric field, which leads to a rather lower conversion of methane. However, the Pd/ $\gamma$ -alumina packed bed reactor shows a better performance compared to the non-packed reactor, as well as compared to the bare  $\gamma$ -alumina packed bed reactor, by improving the  $C_2$  yield, reducing the deposits formation and furthermore increasing the energy efficiency of the plasma reaction. It is important to mention that, in the present study, the formation of deposits was included to the calculation of selectivities for gas hydrocarbons, and therefore, the mass balances were considered in the calculations by reporting the selectivities based on all formed  $C_xH_y$  products, including deposits. The parameters represented in Table 2 indicate the synergy of Pd/ $\gamma$ -alumina and the DBD reactor for conversion of methane to  $C_2$  hydrocarbons, while the yield of deposits was noticeably reduced for the Pd/ $\gamma$ -alumina packed reactor compared to the non-packed reactor and the bare  $\gamma$ -alumina packed reactor.



**Figure 9.** The mechanism of the catalytic coupling of methane to form  $\text{C}_2$  products by interaction of DBD plasma-generated radicals with the surface of Pd/γ-alumina: (a) The radical generation by plasma activation, (b) The adsorption of radicals on the catalyst surface, (c) The surface reactions by interacting with Palladium active sites, (d) The hydrogen attachment and the recombination reactions (e) The desorption of  $\text{CH}_x$  and  $\text{C}_2\text{H}_y$  to gas-phase.



### 3. Materials and Methods

#### 3.1. Materials and Characterizations

The  $\gamma$ -alumina (surface area: 234 m<sup>2</sup>/gr, Alfa Acer), Pd (5 wt%)/ $\gamma$ -alumina (surface area: 157 m<sup>2</sup>/gr, dispersion 24.0%, 4.7 nm Pd particle size, Alfa Acer), Pd (1 wt%)/ $\gamma$ -alumina (surface area: 160 m<sup>2</sup>/gr, dispersion 27.7%, 4.1 nm Pd particle size, Alfa Acer) and Pd (0.5 wt%)/ $\gamma$ -alumina (surface area: 159 m<sup>2</sup>/gr, dispersion 25.3%, 4.4 nm Pd particle size, Alfa Acer) were utilized as the catalyst samples. The surface area of the samples was measured with nitrogen physisorption at 77 K (Surface area and Porosity Analyzer, TriStar, Micrometrics). CO-chemisorption (ChemiSorb 2750, Micrometrics) was utilized to measure the metal dispersion and particle size of the Pd catalysts. The values for the surface area, dispersion and Pd particle size are given above, inside the brackets for each catalyst.

#### 3.2. The Implemented Packed Bed DBD Plasma Reactor and Its Operation

The experiments were performed in a DBD plasma reactor by applying a high voltage of 7–9 kV and the frequency of 23 kHz, where the average output power remained in the range of 7–8 W during the plasma reaction. A mixture of CH<sub>4</sub> and Ar was fed to the inlet of the reactor, containing 5 vol% of CH<sub>4</sub> as the reactant. The DBD plasma reactor was operated at ambient condition. The plasma reaction was initiated at room temperature. The temperature raise during the reaction time was minor. The maximum temperature raise for the outer surface of the plasma reactor was 52 °C after 1 hour of the reaction time. The products were analyzed with a Varian 450 Gas Chromatograph (GC) equipped with Thermal Conductivity Detector (TCD) and Flame Ionization Detector (FID). The details of the DBD plasma reactor, the operation of that and the details of the analysis of the products have been explained in the previous studies of the authors [21]. The following equations were used to calculate the conversion, selectivity and yield of H<sub>2</sub>:

$$\text{Conversion of CH}_4 (\%) = \frac{\text{CH}_4 \text{ converted (mmol/s)}}{\text{CH}_4 \text{ introduced (mmol/s)}} \times 100$$

$$\text{Selectivity of C}_x\text{H}_y \text{ gas phase product } (\%) = \frac{\text{C}_x\text{H}_y \text{ produced (mmol/s)} \times x}{\text{CH}_4 \text{ converted (mmol/s)}} \times 100$$

$$\text{Selectivity of the formed deposits } (\%) = \frac{\text{CH}_4 \text{ converted } \left(\frac{\text{mmol}}{\text{s}}\right) - \text{CH}_4 \text{ consumed to form gas phase products } \left(\frac{\text{mmol}}{\text{s}}\right)}{\text{CH}_4 \text{ converted } \left(\frac{\text{mmol}}{\text{s}}\right)} \times 100$$

$$\text{Hydrogen Yield } (\%) = \frac{\text{H}_2 \text{ produced (mmol/s)}}{2 \times \text{CH}_4 \text{ introduced (mmol/s)}} \times 100$$

### 4. Conclusions

The conversion of methane at ambient conditions was investigated in a DBD plasma–catalyst hybrid system. The Pd/ $\gamma$ -alumina packed reactor showed a synergy between the plasma and the Pd catalyst in improving the yield of C<sub>2</sub> and in substantially reducing the deposits' formation. In addition, the energy efficiency of the Pd/ $\gamma$ -alumina packed reactor was higher than those obtained for the non-packed reactor and the  $\gamma$ -alumina packed reactor. The amount of metal loading of Pd showed a notable effect on the distribution of C<sub>2</sub> products, where low amounts of Pd (0.5 and 1 wt%) were favorable for a higher production of unsaturated compounds (C<sub>2</sub>H<sub>4</sub>, C<sub>3</sub>H<sub>6</sub>). Alkanes (C<sub>2</sub>H<sub>6</sub>, C<sub>3</sub>H<sub>8</sub>) became the main products, by increasing the Pd loading to 5 wt%, lowering the formation of unsaturated compounds. Furthermore, the involved radical chemistry was discussed for the effect of Pd in promoting hydrogenation reactions. It was explained that, for the Pd/ $\gamma$ -alumina packed reactor, the rate of hydrogenation reaction of CH<sub>x</sub> and C<sub>2</sub>H<sub>y</sub> with H radicals on the catalyst surface becomes faster than the rate of their deposition, due to the presence of Palladium.



**Author Contributions:** Conceptualization, M.T.; Methodology, M.T.; Data Curation, M.T.; Formal Analysis, M.T.; Writing—Original Draft, M.T.; Writing—Review and Editing, H.G. and M.T. All authors have read and agreed to the published version of the manuscript.

**Funding:** This research received no external funding.

**Conflicts of Interest:** The authors declare no conflict of interest.

## References

- Kim, H.H.; Teramoto, Y.; Negishi, N.; Ogata, A. A multidisciplinary approach to understand the interactions of nonthermal plasma and catalyst: A review. *Catal. Today* **2015**, *256*, 13–22. [\[CrossRef\]](#)
- Jo, S.; Lee, D.H.; Song, Y.H. Product analysis of methane activation using noble gases in a non-thermal plasma. *Chem. Eng. Sci.* **2015**, *130*, 101–108. [\[CrossRef\]](#)
- Neyts, E.C. Plasma-Surface Interactions in Plasma Catalysis. *Plasma Chem. Plasma Process.* **2016**, *36*, 185–212. [\[CrossRef\]](#)
- Zeng, Y.X.; Wang, L.; Wu, C.F.; Wang, J.Q.; Shen, B.X.; Tu, X. Low temperature reforming of biogas over K-, Mg- and Ce-promoted Ni/Al<sub>2</sub>O<sub>3</sub> catalysts for the production of hydrogen rich syngas: Understanding the plasma-catalytic synergy. *Appl. Catal. B Environ.* **2018**, *224*, 469–478. [\[CrossRef\]](#)
- Rueangjitt, N.; Sreethawong, T.; Chavadej, S.; Sekiguchi, H. Non-Oxidative Reforming of Methane in a Mini-Gliding Arc Discharge Reactor: Effects of Feed Methane Concentration, Feed Flow Rate, Electrode Gap Distance, Residence Time, and Catalyst Distance. *Plasma Chem. Plasma Proc.* **2011**, *31*, 517–534. [\[CrossRef\]](#)
- Wang, B.; Guan, H.M. Highly Efficient Conversion of Methane to Olefins via a Recycle-Plasma-Catalyst Reactor. *Catal. Lett.* **2016**, *146*, 2193–2199. [\[CrossRef\]](#)
- Kasinathan, P.; Park, S.; Choi, W.; Hwang, Y.; Chang, J.; Park, Y. Plasma-Enhanced Methane Direct Conversion over Particle-Size Adjusted MO<sub>x</sub>/Al<sub>2</sub>O<sub>3</sub> (M = Ti and Mg) Catalysts. *Plasma Chem. Plasma Proc.* **2014**, *34*, 1317–1330. [\[CrossRef\]](#)
- Górska, A.; Krawczyk, K.; Jodzis, S.; Schmidt-Szałowski, K. Non-oxidative methane coupling using Cu/ZnO/Al<sub>2</sub>O<sub>3</sub> catalyst in DBD. *Fuel* **2011**, *90*, 1946–1952. [\[CrossRef\]](#)
- Kim, J.; Abbott, M.S.; Go, D.B.; Hicks, J.C. Enhancing C–H Bond Activation of Methane via Temperature-Controlled, Catalyst–Plasma Interactions. *ACS Energy Lett.* **2016**, *1*, 94–99. [\[CrossRef\]](#)
- Kim, S.; Kwon, B.; Kim, J. Plasma catalytic methane conversion over sol–gel derived Ru/TiO<sub>2</sub> catalyst in a dielectric-barrier discharge reactor. *Catal Commun.* **2007**, *8*, 2204–2208. [\[CrossRef\]](#)
- Tang, Y.; Zhuo, J.; Cui, W.; Li, S.; Yao, Q. Enhancing ignition and inhibiting extinction of methane diffusion flame by in situ fuel processing using dielectric-barrier-discharge plasma. *Fuel Process. Technol.* **2019**, *194*, 106128. [\[CrossRef\]](#)
- Van Laer, K.; Bogaerts, A. How bead size and dielectric constant affect the plasma behaviour in a packed bed plasma reactor: A modelling study. *Plasma Process Polym.* **2017**, *14*, 1600129. [\[CrossRef\]](#)
- Nozakia, T.; Okazaki, K. Non-thermal plasma catalysis of methane: Principles, energy efficiency, and applications. *Catal. Today* **2013**, *211*, 29–38. [\[CrossRef\]](#)
- Li, X.S.; Zhu, A.M.; Wang, K.J.; Xu, Y.; Song, Z.M. Methane conversion to C<sub>2</sub> hydrocarbons and hydrogen in atmospheric non-thermal plasmas generated by different electric discharge techniques. *Catal. Today* **2004**, *98*, 617–624. [\[CrossRef\]](#)
- Jo, S.; Lee, D.H.; Kang, W.S.; Song, Y.H. Methane activation using noble gases in a dielectric barrier discharge reactor. *Phys. Plasmas* **2013**, *20*, 083509. [\[CrossRef\]](#)
- Sentek, J.; Krawczyk, K.; Młotek, M.; Kalczyńska, M.; Kroker, T.; Kolb, T.; Schenk, A.; Gericke, K.H.; Schmidt-Szałowski, K. Plasma-catalytic methane conversion with carbon dioxide in dielectric barrier discharges. *Appl. Catal. B Environ.* **2010**, *94*, 19–26. [\[CrossRef\]](#)
- Jo, S.; Kim, T.; Lee, D.H.; Kang, W.S.; Song, Y.H. Effect of the Electric Conductivity of a Catalyst on Methane Activation in a Dielectric Barrier Discharge Reactor. *Plasma Chem. Plasma Process.* **2014**, *34*, 175–186. [\[CrossRef\]](#)
- Khalifeh, O.; Taghvaei, H.; Mosallanejad, A.; Rahimpour, M.R.; Shariati, A. Extra pure hydrogen production through methane decomposition using nanosecond pulsed plasma and Pt-Re catalyst. *Chem. Eng. J.* **2016**, *294*, 132–145. [\[CrossRef\]](#)

19. Kim, S.; Choi, J.; Kim, J.; Lee, H.; Song, H.K. Plasma catalytic reaction of methane over nanostructured Ru/-Al<sub>2</sub>O<sub>3</sub> catalysts in dielectric-barrier discharge. *J. Ind. Eng. Chem.* **2005**, *11*, 533–539.
20. Lu, J.; Li, Z. Conversion of natural gas to C<sub>2</sub> hydrocarbons via cold plasma technology. *J. Nat. Gas Chem.* **2010**, *19*, 375–379. [[CrossRef](#)]
21. Taheraslani, M.; Gardeniers, H. Coupling of CH<sub>4</sub> to C<sub>2</sub> Hydrocarbons in a Packed Bed DBD Plasma Reactor: The Effect of Dielectric Constant and Porosity of the Packing. *Energies* **2020**, *13*, 468. [[CrossRef](#)]
22. Mei, D.; Zhu, X.; He, Y.L.; Yan, J.D.; Tu, X. Plasma-assisted conversion of CO<sub>2</sub> in a dielectric barrier discharge reactor: Understanding the effect of packing materials. *Plasma Sources Sci. Technol.* **2015**, *24*, 015011. [[CrossRef](#)]
23. Butterworth, T.; Allen, R.W.K. Plasma-catalyst interaction studied in a single pellet DBD reactor: Dielectric constant effect on plasma dynamics. *Plasma Sources Sci. Technol.* **2017**, *26*, 065008. [[CrossRef](#)]
24. Belov, I.; Paulussen, S.; Bogaerts, A. Appearance of a conductive carbonaceous coating in a CO<sub>2</sub> dielectric barrier discharge and its influence on the electrical properties and the conversion efficiency. *Plasma Sources Sci. Technol.* **2016**, *25*, 015023. [[CrossRef](#)]
25. Chandrashekaraiyah, T.H.; Bogdanowicz, R.; Rühl, E.; Danilov, V.; Meichsner, J.; Thierbach, S.; Hippler, R. Spectroscopic Study of Plasma Polymerized a-C:H Films Deposited by a Dielectric Barrier Discharge. *Materials* **2016**, *9*, 594. [[CrossRef](#)]
26. Gadzhieva, N.N. Methane Adsorption and Plasma-Assisted Catalytic Conversion on the Surface of  $\gamma$ -Alumina. *High Energy Chem.* **2003**, *37*, 38–43. [[CrossRef](#)]
27. Nozaki, T.; Muto, N.; Kado, S.; Okazaki, K. Dissociation of vibrationally excited methane on Ni catalyst: Part 1. Application to methane steam reforming. *Catal. Today* **2004**, *89*, 57–65. [[CrossRef](#)]
28. Puliyalil, H.; Jurković, D.L.; Dasireddy, V.D.B.C.; Likoza, B. A review of plasma-assisted catalytic conversion of gaseous carbon dioxide and methane into value-added platform chemicals and fuels. *RSC Adv.* **2018**, *8*, 27481–27508. [[CrossRef](#)]
29. Correale, G.; Winkel, R.; Kotsonis, M. Energy deposition characteristics of nanosecond dielectric barrier discharge plasma actuators: Influence of dielectric material. *J. Appl. Phys.* **2015**, *118*, 083301. [[CrossRef](#)]
30. Taheraslani, M.; Gardeniers, H. High-Resolution SEM and EDX Characterization of Deposits Formed by CH<sub>4</sub>+Ar DBD Plasma Processing in a Packed Bed Reactor. *Nanomaterials* **2019**, *9*, 589. [[CrossRef](#)]
31. Cho, W.; Baek, Y.; Chaikim, Y.; Anpo, M. Plasma catalytic reaction of natural gas to C<sub>2</sub> product over Pd-NiO/Al<sub>2</sub>O<sub>3</sub> and Pt-Sn/Al<sub>2</sub>O<sub>3</sub> catalysts. *Res. Chem. Intermed.* **2002**, *28*, 343–357. [[CrossRef](#)]
32. Tu, X.; Gallon, H.J.; Twigg, M.V.; Gorrie, P.A.; Whitehead, J.C. Dry reforming of methane over a Ni/Al<sub>2</sub>O<sub>3</sub> catalyst in a coaxial dielectric barrier discharge reactor. *J. Phys. D Appl. Phys.* **2011**, *44*, 274007. [[CrossRef](#)]
33. Tu, X.; Gallon, H.J.; Whitehead, J.C. Plasma-assisted reduction of a NiO/Al<sub>2</sub>O<sub>3</sub> catalyst in atmospheric pressure H<sub>2</sub>/Ar dielectric barrier discharge. *Catal. Today* **2013**, *211*, 120–125. [[CrossRef](#)]
34. De Bie, C.; Verheyde, B.; Martens, T.; van Dijk, J.; Paulussen, S.; Bogaerts, A. Fluid Modelling of the Conversion of Methane into Higher Hydrocarbons in an Atmospheric Pressure Dielectric Barrier Discharge. *Plasma Process. Polym.* **2011**, *8*, 1033–1058. [[CrossRef](#)]
35. Kado, S.; Urasaki, K.; Sekine, Y.; Fujimoto, K.; Nozaki, T.; Okazaki, K. Reaction mechanism of methane activation using non-equilibrium pulsed discharge at room temperature. *Fuel* **2003**, *82*, 2291–2297. [[CrossRef](#)]
36. Bae, J.; Lee, M.; Park, S.; Hong, M.G.J.D.Y.; Kim, Y.D.; Park, Y.K.; Hwang, Y.K. Investigation of intermediates in non-oxidative coupling of methane by non-thermal RF plasma. *Catal. Today* **2017**, *293*, 105–112. [[CrossRef](#)]
37. Tomaszewska, A.; Stępień, Z.M. The influenced of the external electric field on the hydrogen-palladium system. *J. Phys.* **2007**, *79*, 012028. [[CrossRef](#)]

